

# Static and seismic design of Dry Stone Retaining Walls (DSRWs) following Eurocode standards

Nathanaël Savalle<sup>a,b,\*</sup>, Christine Monchal<sup>c</sup>, Eric Vincens<sup>d</sup>, Sten Forcioli<sup>c</sup>, Paulo B. Lourenço<sup>a</sup>

<sup>a</sup> University of Minho, ISISE, Department of Civil Engineering, Guimarães, Portugal

<sup>b</sup> Université Clermont Auvergne, Clermont Auvergne INP, CNRS, Institut Pascal, F-63000 Clermont-Ferrand, France

<sup>c</sup> Géolithe<sup>1</sup> – Grenoble, 181 rue des Bécasses, 38920 Crolles, France

<sup>d</sup> Ecole Centrale de Lyon, LTDS UMR-CNRS 5513, Université de Lyon, 36 Avenue Guy de Collongue, 69134 Ecully, France

## ARTICLE INFO

### Keywords:

Masonry  
Dry stone  
Retaining walls  
Pseudo-static  
Earthquakes  
Coulomb's wedge  
Standards

## ABSTRACT

Dry Stone Retaining Walls are structures made of rubble stones assembled without mortar and have been present worldwide for centuries. Today, they still constitute an attractive alternative to building techniques involving higher embodied energy, such as reinforced concrete walls. This study uses a pseudo-static approach to give design recommendations to maintain this built heritage and allow its modern construction. Both non-seismic (Eurocode 7) and seismic (Eurocode 8) cases are addressed. The present work confirms that a seismic design is not critical and is therefore not required for zones with a design acceleration below 0.05g. In addition, this work highlights the significant positive effect of the stone bed inclination and the internal wall face batter. Finally, depending on the wall site conditions and the seismic zone associated with the project, general design recommendations are given to optimise the volume of stones used, which are illustrated in the case of France. These recommendations based on pseudo-static analyses are already usable in practice for low to moderate seismic areas as the required retaining wall dimensions can be easily implemented on-site. In addition, it is also shown that the actual French recommendations for these walls fully comply with Eurocode 7.

## 1. Introduction

Dry stone structures have been built in most regions of the world, sometimes shaping typical and valuable landscapes. These vernacular structures are made of rubble stones carefully assembled by hand and without mortar. Dry Stone Retaining Walls (DSRWs) are likely to constitute the most representative part of this built heritage, allowing agricultural activities on terraces and traffic on rural roads in mountainous or sloped areas. Therefore, DSRWs play an essential economic role in these regions that benefit less from globalisation and major investments. In addition, they also hold a high cultural value, sometimes labelled by UNESCO (e.g., Douro's Valley in Portugal or the Lavaux's Terraces in Switzerland). In fact, the art of dry stone walling, knowledge and techniques were designated as Intangible Cultural Heritage of Humanity by UNESCO in 2018. However, these structures have often faced a lack of maintenance in recent decades and require urgent repair.

Given the need to preserve and repair old DSRWs, several research

studies have been conducted mainly in Europe. Experimental works [1–3], analytical [4–7] and numerical studies [8–15] focused on the static mechanical behaviour of 2D sloped DSRWs, while other studies investigated the 3D mechanical behaviour of these walls in case of a concentrated traffic load [16–19]. In France, these researches led to two practical handbooks that include design rules for DSRWs retaining slopes. These are valid for any country with similar building techniques, which can be found worldwide [20,21]. However, even though the recommendations are used in practice and recognised by the drystone masonry and civil engineering communities, they do not consider seismic action. Only a few study cases have been investigated according to the past French seismic recommendations [22,23]. Moreover, the validation of the recommendations according to Eurocode 7 [24–26] has not been investigated exhaustively, even if partly considered in the latest DSRWs French handbook [21].

To address the seismic design of DSRWs in slopes, the authors developed a pseudo-static analytical tool based on Coulomb's wedge

\* Corresponding author.

E-mail addresses: [n.savalle@civil.uminho.pt](mailto:n.savalle@civil.uminho.pt) (N. Savalle), [christine.monchal@geolithe.com](mailto:christine.monchal@geolithe.com) (C. Monchal), [eric.vincens@ec-lyon.fr](mailto:eric.vincens@ec-lyon.fr) (E. Vincens), [sten.forcioli@geolithe.com](mailto:sten.forcioli@geolithe.com) (S. Forcioli), [pbl@civil.uminho.pt](mailto:pbl@civil.uminho.pt) (P.B. Lourenço).

<sup>1</sup> <http://www.geolithe.fr/ingenieurs-conseils/>.

theory, which was validated by pseudo-static scaled-down laboratory experiments [27]. The first section of this paper revises the analytical method, while the second section provides a comparison with the current standards on geotechnical engineering and seismic engineering, Eurocode 7 & 8, respectively [24–26,28,29]. Finally, following the Eurocodes, recommendations are given for designing DSRWs in areas ranging from very low to high seismicity.

## 2. Analytical method

The analytical method relies on the limit-equilibrium theory under plane strain conditions (Fig. 1). The DRSW is characterised by a height  $H$ , a base width  $B$ , an external slope to the vertical of  $\lambda_e$  and an internal slope to the vertical of  $\lambda_m$ . The bed inclination of the wall is referred to as  $\alpha$  and the backfill slope as  $\beta$ . Contrary to the static limit-equilibrium approach of Villemus [30], the analytical method includes seismic forces modelled as equivalent horizontal pseudo-static actions. Briefly, the pseudo-static equilibrium of a Coulomb’s wedge of soil is first computed to obtain the pseudo-static active earth pressure [31–33]. The wall’s equilibrium is then computed, stating the possible types of failure: an internal sliding or toppling mode [34].

Fig. 2 describes the backfill-wall system, with all geometrical and mechanical parameters clarified. The wall is characterised by a homogeneous medium (Fig. 1) with its homogeneous unit weight  $\gamma_{rw}$  (accounting for voids between stones) and joint frictional angle  $\varphi_{rw}$ . Similarly, the backfill is modelled as a homogeneous medium described by its unit weight  $\gamma_f$ , cohesion  $C_f$  and friction angle  $\varphi_f$ . Compared to other retaining structures, the particularity of DSRWs lies in a failure line developing through the dry joints, which is modelled as an equivalent straight failure line with an inclination  $\omega$  (Fig. 1). In practice, the inclination of this failure line from the bed joints is limited by a maximum value of approximately 20°, see details in [27]. This inclination is also different from the homogenised inclination  $\theta$  of the failure line crossing the backfill, which mainly depends on material (soil friction and cohesion), geometrical (slope of the backfill) and seismic (pseudo-static accelerations) parameters, as explained below.

The mechanical system has three unknowns ( $\theta$ ,  $\omega$  and  $h_b$ ) that should be determined to compute the earth pressure  $F_\delta$ . According to the Coulomb soil’s wedge theory, for each combination of these parameters, the limit equilibrium of the soil’s wedge  $D_1D_2D_3$  can be calculated (Fig. 2b-c) to evaluate the active earth pressure  $F_\delta$ . In particular, the weight  $P_f$  of the soil is proportional to the wedge area (triangle  $D_1D_2D_3$ ) and is applied at the gravity centre of the triangle  $D_1D_2D_3$ . Similarly, the pseudo-static action (inertial force due to the seismic motion)  $F_f$  is also proportional to the wedge area and applied at its gravity centre. The

backfill frictional reaction  $R_p$ , application point and intensity are unknown, but its orientation is given by the backfill friction angle  $\varphi_f$  since the limit-equilibrium is assumed. Similarly, the orientation, yet not the application point, of the backfill cohesive reaction  $R_C$  is known. Regarding the backfill-wall interface, the interface cohesive reaction  $R_{Cint}$  has an unknown point of application and a known orientation. The intensities of the cohesive forces ( $R_C$  and  $R_{Cint}$ ) are proportional to the cohesive strength and the length of the interface ( $D_1D_3$  and  $D_1D_2$ ). Hereafter, the interface cohesive strength ( $R_{Cint}$ ) always equals zero, as the drain directly behind a DSRW is usually made of dry cohesionless gravel.

Finally, the earth pressure  $F_\delta$  has a known orientation  $\delta$  (internal face of the wall) and application point but unknown intensity. The intensity is deduced from the mechanical equilibrium of the soil’s wedge (Fig. 2c). In the absence of pseudo-static action  $F_f$  and cohesive resistance, the application point of the earth pressure is located at one-third of the height of the retaining structure. Then, adding cohesive effects decrease the application point height while adding a pseudo-static action increases its height. The reader can refer to the literature for deeper insights into the location of the application point of earth pressure in this case [34–36].

The analytical method also accounts for the tensile cracks that classically occur at the top of cohesive backfill and reduce the cohesive forces ( $R_C$  and  $R_{Cint}$ ). In addition, in the present work, the presence of dead loads on top of the backfill and saturated retained backfill [34] can be accounted for, yet not described here for brevity.

In a second stage of the calculation, the equilibrium of the wall itself is computed (Fig. 3) including its own weight and the pseudo-static horizontal action, applied at the centre of gravity of the studied portion of wall  $A_2A_3D_1E$ , corresponding to the part above the failure line  $D_1E$ . The interface actions  $F_\delta$  and  $R_{Cint}$  (as well as their line of actions) are derived from the previous stage of calculation. Subsequently, the wall equilibrium is computed in the  $X$  and  $Y$  directions to evaluate the base reaction  $R_b$ . The equilibrium in terms of momentum gives the application point of  $R_b$ . Finally, the stability of wall portion  $A_2A_3D_1E$  is computed considering a toppling mode of failure (e.g. application point inside the wall, i.e.  $l_b > 0$ , or any other criteria defined in the following sections) or a sliding mode of failure. For this last point, the base reaction  $R_b$  is projected on the plane defined by the orientation of the bed joints (axes  $X_s$  and  $Y_s$  in Fig. 3), and then Mohr-Coulomb criterion is checked. Note that the bed joints’ orientation is updated because of the possible internal rotation of stones inside DSRWs (see [34] for more details). Finally, the unknowns of the system ( $\theta$ ,  $\omega$  and  $h_b$ ) are optimised for each failure mode to find the most critical situation for the criterion checked. Several automated iterations involving the base width  $B$  of the

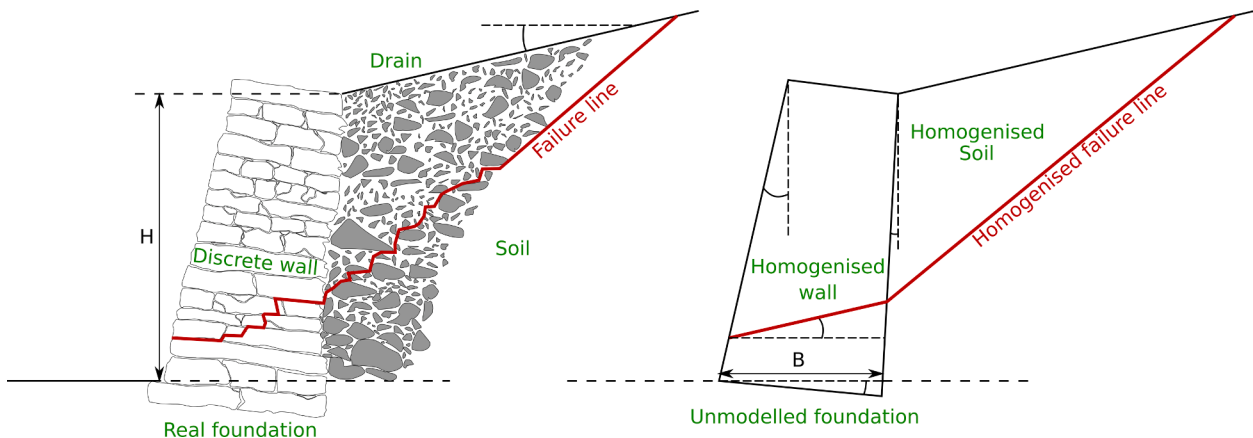


Fig. 1. DSRW with its geometric parameterisation a): actual backfill-wall system; b): modelled backfill-wall system. The present sign convention makes the internal batter ( $\lambda_m$ ) negative.

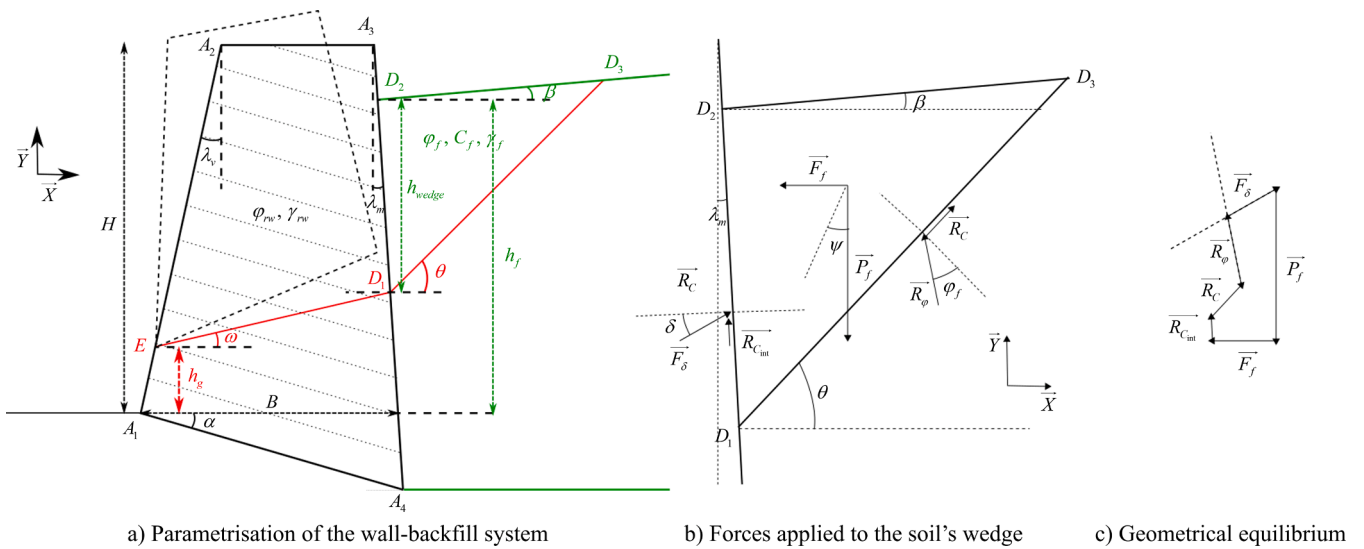


Fig. 2. Parametrisation of the mechanical system and geometrical equilibrium of the soil's wedge in order to compute the earth pressure  $F_s$ . [34].

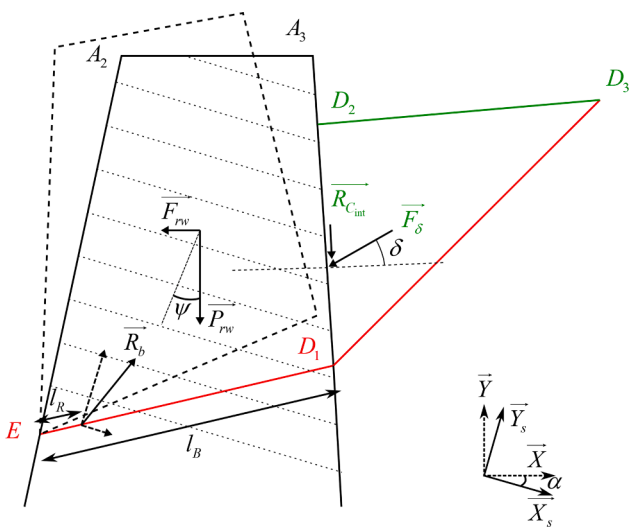


Fig. 3. Equilibrium of the dry stone retaining wall [34].

wall allows to identify the minimum  $B$  value that barely satisfies the stability criteria.

The method has been validated on scaled pseudo-static experiments on a tilting table, using dry joint brick retaining walls retaining a sandy backfill [27]. Fig. 4 gives the results, showing that the developed

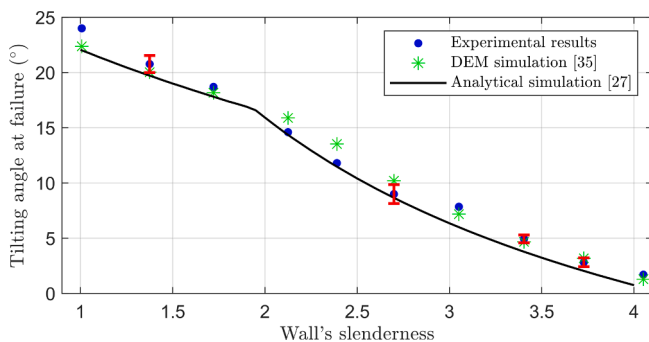


Fig. 4. Comparison of DEM simulation, analytical simulation and experimental tilting tests [37].

pseudo-static approach is as precise as more sophisticated Discrete Element Modelling (DEM) simulations [37].

As additional validation, the analytical method was used to model two sets of experimental campaigns carried out on full-scale DSRWs with 1) a hydrostatic load [1]; 2) a dry backfill load, as displayed in Fig. 5 [2,3]. Table 1 describes the geometric and mechanical parameters of the experiments, along with the analytical results, which are in excellent agreement for both campaigns. Moreover, the developed analytical approach provides a similar level of accuracy to the results of Villemus et al. [1] and Colas et al. [6,38].

### 3. Design of DSRWs following Eurocodes

The present section aims at designing DSRWs using the analytical method and the partial safety factors (actions, material properties and resistance) from Eurocode 7 and 8 [24–26,28]. First, it is emphasised that in a seismic context, a pseudo-static method (like the one presented above) will never accurately predict the true time evolution of the dynamic response or resistance of a real DSRW during an earthquake. Therefore, it is only used as a simplified design method proposed by Eurocode 8 to give fast seismic assessment of retaining walls. No partial safety factor related to the method is considered since no constant bias



Fig. 5. Experimental toppling failure obtained by Colas [39].

**Table 1**

Parameters of the full-scale DSRWs experimental campaigns from [1–3]. Experimental and analytical results are also given.

Name*	V1l	V2l	V3l	V4l	V5s	C1g†	C2s	C3s	C4l
<b>Geometrical parameters</b>									
Height H (m)	2	1.95	4	2	4.25	2.5	2.5	2.5	2.5
Base width B (m)	0.9	0.91	1.8	0.9	1.8	0.6	0.6	0.7	0.65
External batter $\lambda_v$ (%)	15	0	15	12	15	6	6	6	6
Stone bed inclination $\alpha$ (°)	0	0	0	4	8.5	3.4	3.4	9.1	9.1
Backfill slope $\beta$ (°)	NA	NA	NA	NA	NA	26.4	31.7	32.6	34.9
<b>Mechanical parameters</b>									
Wall unit weight $\gamma_{rw}$ (kN/m <sup>3</sup> )	15.4	14.9	15.7	15.7	18.0	21.0	20.0	20.0	21.8
Blocks friction $\phi_{rw}$ (°)	36	36	36	36	28.5	27	25	25	35
Internal rotation (°)‡	5	5	5	5	5	5	5	5	5
Backfill unit weight $\gamma_f$ (kN/m <sup>3</sup> )	NA	NA	NA	NA	NA	14.9	14.9	14.9	14.9
Backfill friction $\phi_f$ (°)	NA	NA	NA	NA	NA	37.7	37.7	37.7	37.7
<b>Experimental results</b>									
Critical height (m)	1.74	1.9	3.37	1.94	3.62	>2.17	2.41	2.96	2.95
Failure mode (S/T)	S	S/T	S	S/T	S	NA	S/T	T	T
<b>Analytical results</b>									
Critical height (m)	1.73	1.84	3.48	1.86	3.68	2.86	2.69	3.02	2.82
Failure mode (S/T)§	S	S/T	S	S/T	S	T	S/T	T	T
Difference to exp.	-1%	-3%	+3%	-4%	+2%	NA	+11%	+2%	-4%

\* V refers to Villemus [1] with hydrostatic loading and C to Colas [2,3] with backfill loading, while l refers to limestone blocks, s to schist blocks and g to granite blocks.

† This experiment failed. However, the wall resisted at least a loading corresponding to a backfill height of 2.17m.

‡ This information is based on experimental results, using a default value. Details can be found in [1–3] for the experiments and in [34,40] for the analytical method.

§ A combined sliding-overturning failure has been defined if the critical theoretical heights of the two failure modes were within a range of  $\pm 5\%$ .

**Table 2**

Partial safety factors for non-seismic and seismic safety verifications; Annex A of the Eurocode 7 [24] and ENTPE (Eds.) et al. [21].

	Eurocode 7 [24]			SLS	French professional rules [21]
	ULS				
	EQU	STR/GEO	SEISM		
<b>Safety factors for actions</b>					
Favourable weight actions factor ( $\gamma_{G, fav}$ )	0.9	1	1	1	1
Unfavourable weight actions factor ( $\gamma_{G, unfav}$ )	1.1	1.35	1	1	1.35
<b>Safety factors for material properties</b>					
Drained soil friction angle factor ( $\gamma_{\phi}$ )	1.25	1	1.25	1	1
Drained soil cohesion factor ( $\gamma_{c'}$ )	1.25	1	1.25	1	1.25
<b>Safety factors for resistances</b>					
Sliding factor ( $\gamma_{R, h}$ )	1	1.1	1	NA	1
Toppling factor ( $\gamma_{R, v}$ )	1	NA	1	NA	1
Eccentricity factor ( $1 - 2e/B$ )	NA	1/15	NA	1/2	1
Model resistant factor ( $\gamma_{R, d}$ )	1	1	1	1	1.2

has been found in the validation processes between theoretical and experimental results. Moreover, only the wall’s internal sliding and toppling failures are considered: the bearing capacity of the foundation soil at ultimate or serviceability limit states are assumed not to be reached. Similarly, the passive soil is considered infinitely rigid, which is reasonable according to Alejano et al. [5]. Finally, liquefaction and the failure of the entire soil slope are disregarded. Table 2 presents the safety factors used for the computations as well as those from the French professional rules, which are similar [21].

Regarding non-seismic verifications, the Ultimate Limit State Equilibrium (ULS EQU), the Structural/Geotechnical Ultimate Limit State with the second approach (ULS STR/GEO), see [41], and the Serviceability Limit State (SLS) are examined. The Ultimate Limit State (ULS SEISM) is applied for the seismic verification.

For the toppling verification of the SLS and the ULS STR/GEO, the design criterion to satisfy corresponds to the maximum eccentricity (noted  $e$ ) of the transmitted load through the wall, as stated in Eurocode 7 [25,26]. In the context of the ULS EQU and SEISM verifications, the partial safety factors  $\gamma_m$  ( $\gamma_{\phi}$  and  $\gamma_{c'}$ ) for the materials are only applied to the backfill soil properties and not to the friction between blocks (as mentioned in [41–43]). The friction between blocks is linked to the wall resistance, thus to the resistance safety factor  $\gamma_R$ . As a consequence, applying a safety factor for the block material (block-block friction)

would penalise twice the same parameters, which is not in agreement with the framework of Eurocodes. Moreover, in the seismic verification (ULS SEISM), the safety factors for materials are linked to the degradation of the shear strength of soils at high strain and/or in the presence of pore pressures. These are unlikely to occur for dry block-block joints [42–44].

### 3.1. Non-seismic case

Computations discarding the seismic action are carried out on five walls, whose main characteristics are presented in Table 3. The walls are built of stones with geological natures representative of European and, in particular French, geology (molasse or marl sandstone, schist, limestone and granite). They include typical variations of essential DSRW properties (geometrical shape and soil resistance). Note that their height is typical of relatively high DSRWs. The backfill-wall interface friction angle  $\delta$  is equal to the soil friction angle, given the dry gravel drain placed behind each DSRW [2,3]. Both the internal batter  $\lambda_m$  and the stone bed inclination  $\alpha$  are initially equal to zero. The minimum required (bottom) widths for the walls given by the Eurocodes are then computed and compared to the recommended widths from ENTPE (Eds) et al. [21].

The recommendations from ENTPE (Eds) et al. [21] are very close to the maximum value recommended by the Eurocode standards with

**Table 3**

Main characteristics and required widths of five typical DSRWs according to Eurocode 7 (non-seismic case) criteria; maximum values are given in bold. Comparisons with the recommendations of ENTPE (Eds) *et al.* [21] are also given. Each column heading displays the critical failure mode (T: toppling; S: sliding). Granite DSRWs have similar properties as schist walls, and the values shown for schist can be used.

	Wall 1 (T) Molasse	Wall 2 (S) Schist	Wall 3 (T) Limestone	Wall 4 (S) Schist	Wall 5 (T) Limestone
<b>Mechanical &amp; geometric properties</b>					
Height H (m)	2.5	2.5	2.5	2.5	2.5
External batter $\lambda_p$ (%)	0	10	20	10	0
Backfill slope $\beta^*$ (°)	0	0	0	0	10
Wall unit weight $\gamma_{rw}$ (kN/m <sup>3</sup> )	16	20	20	20	20
Blocks friction $\phi_{rw}$ (°)	36	28	36	28	36
Backfill unit weight $\gamma_f$ (kN/m <sup>3</sup> )	20	20	20	20	20
Backfill cohesion $C_f$ (kPa)	0	0	0	5	0
Backfill friction $\phi_f$ (°)	30	30	25	25	30
Interface friction $\delta$ (°)	30	30	25	25	30
<b>Non-seismic design: wall base widths</b>					
ULS EQU (Sliding)	0.57m	<b>0.83m</b>	0.85m	<b>0.68m</b>	0.54m
ULS EQU (Toppling)	<b>0.83m</b>	0.77m	<b>0.90m</b>	0.51m	<b>0.81m</b>
ULS STR-GEO (Sliding)	0.51m	0.77m	0.82m	0.63m	0.47m
ULS STR-GEO (Toppling)	0.76m	0.71m	0.84m	0.30m	0.74m
SLS (Eccentricity)	<b>0.89m</b>	0.78m	<b>0.91m</b>	0.30m	<b>0.86m</b>
ENTPE (Eds) et al. [21]	<b>0.91m</b>	<b>0.85m</b>	<b>1.00m</b>	<b>0.75m</b>	<b>0.88m</b>
Absolute difference	2%	2%	9%	9%	2%

\* The slope inclination (backfill slope) refers to the backfill directly retained by the wall and not the global slope of the site.

slightly larger and conservative values: on average + 5% and maximum + 10 % difference. The most critical limit state and the corresponding failure mode differ according to the studied walls, justifying the consideration of all possible limit states. Finally, even if only five case studies are shown for brevity, the authors carried out a more comprehensive set of typical walls with identical conclusions.

### 3.2. Seismic case

#### 3.2.1. Global analysis

The same walls are assessed according to Eurocode 8 [29,44], assuming their design is provided by the most non-seismic critical case mentioned above. Keeping all other geometrical parameters constant, the extra-width required to withstand the seismic loading is computed (see Table 2 for the associated partial safety factors). Here, the authors recall that this section does not aim to describe precisely the dynamic behaviour of DSRWs against earthquakes but aims to provide a safe design width for DSRWs built in a seismic context. For this reason, the simplified pseudo-static modelling strategy is considered. The following equations give the pseudo-static design accelerations (horizontal  $a_h$  and vertical  $a_v$ ) [29]:

$$a_h = \frac{a_{gR} * S^* S_T * \gamma_I}{r}, \quad a_v = 0.5 * a_h \tag{1}$$

where  $a_{gR}$  is the reference acceleration for the considered seismic zone; S is the soil amplification factor (the maximum value being  $S = 1.8$ );  $S_T$  is the topographic amplification coefficient;  $\gamma_I$  is the importance coefficient of the structure; and  $r$  is the seismic behaviour factor [29]. The latter parameter considers the wall's ability to move during the seismic motion and dissipate seismic energy before collapsing [28,44].

Scaled-down experiments on a shaking table suggested a conservative value of  $r = 1.5$  [45], corresponding to walls able to handle small movements before collapsing according to Eurocode 8 [28]. In addition, numerical simulations using DEM approach have concluded that  $r = 1.5$  was indeed conservative enough for the French seismicity [46]. In fact, after a numerical validation step using scaled-down experiments with dynamic time-history analyses, the numerical model was applied to full-

scale structures with various dynamic time-history analyses (signal and backfill-wall parameters). Then, comparing the obtained numerical resistance and the estimated (analytical) pseudo-static resistance, the seismic behaviour factor  $r$  for each configuration was determined. Combining all the results, a mean value of  $r = 2.0$  and a minimum value of  $r = 1.8$  have been found. Therefore, a conservative recommended value of  $r = 1.5$  was proposed since Eurocode only advises three values for  $r$  namely 1, 1.5 and 2. Even though this study has focused on the French case with moderate seismicity, the obtained outcome is considered acceptable elsewhere in Europe, especially given the safety margin taken at each step in [46]. In all analyses, the studied DSRWs are assumed to belong to the normal importance class. Particular conditions that rarely occur on-site are excluded (e.g., walls near very high buildings, highways, hospitals or energy facilities). It means that the importance coefficient  $\gamma_I$  is lower than (or equal to) 1, which also implies no topographic amplification ( $S_T = 1$ ). Depending on the reference acceleration  $a_{gR}$ , the most critical design condition reads:

$$a_{h,max} = \frac{a_{gR} * 1.8}{1.5} = a_{gR} * 1.2, \quad a_{v,max} = 0.5 * a_{h,max} = a_{gR} * 0.6 \tag{2}$$

Fig. 6 depicts the extra-width required to fulfil a seismic design compared to the previously non-seismic design for each of the five walls (Table 3). Eurocode 8 states that seismic design is not required below a threshold of  $a_h = 0.05g$  [29]: actually, the current calculations show that even if accounted for, the seismic case is not critical for the wall stability (Fig. 6). For higher design accelerations, walls sensitive to a sliding failure (case of schist wall, Fig. 6a) tend to have larger required extra-widths than those sensitive to a toppling failure (Fig. 6b-c). Finally, for high seismic hazard regions in Europe and France, see Fig. 7 ( $a_h = 0.25 - 0.4g$ ), extra-widths reach very high values (+200%), reflecting the inadequacy of the pseudo-static method for high reference accelerations, which may provide unpractical recommendations for on-site works. Here, it is noted that wall disintegration is not considered, meaning that in high seismicity areas, additional prevention actions may be required.

A larger set of walls was analysed to obtain more general results. Walls geometries are still given in Table 3, but each geometry uses three different types of stone (schist, limestone, and molasse). Additionally, the analysis considers three typical bed inclinations  $\alpha$  ( $0^\circ$ ,  $10\% = 5.7^\circ$  and  $20\% = 11.3^\circ$ ) for each wall to improve the sliding resistance of DSRWs [2,30,47,48]. Fig. 8 gives the maximum (and mean) required extra-widths for DSRWs built with different kinds of stone depending on the stone bed inclination  $\alpha$ . Here, the local peaks are related to vertical asymptotes for a peculiar response: when the design acceleration  $a_h$  equals  $a_{h,critical}$  (Eq. (3)), the whole retained soil slope loses its static equilibrium leading to infinite forces impossible to be sustained by the wall. Hence, the pseudo-static design requires huge wall widths close to this critical acceleration.

$$a_{h,critical} = \frac{\sin(\varphi_r - \beta) + \frac{C_r \cos \varphi}{\gamma_r * H \cos \beta}}{\cos(\varphi_r - \beta) + 0.5 * \sin(\varphi_r - \beta)} \tag{3}$$

For clarity, the maximum and mean values displayed in Fig. 8 ignore walls around and after their critical acceleration  $a_{h,critical}$ , yet still resulting in small visible local peaks. For example, the first peaks for a design acceleration of about 0.22g observed in Fig. 8 correspond to Wall 5, the only case with a non-zero backfill slope  $\beta$ . Therefore, in practice, one may prefer to build a higher wall with a flat retained backfill than a smaller wall with an inclined backfill, especially in high seismic hazard regions. Finally, Eq. (3) highlights the inherent limitation of the design approach proposed by Eurocodes, which does not apply for high design acceleration  $a_h$ , basically larger than 0.25–0.4g depending on the parameters of the backfill.

Analysing Fig. 8, it is noted that increasing the stone bed inclination is very efficient in reducing the extra-widths according to a pseudo-static design, although this parameter was not integrated into the non-seismic

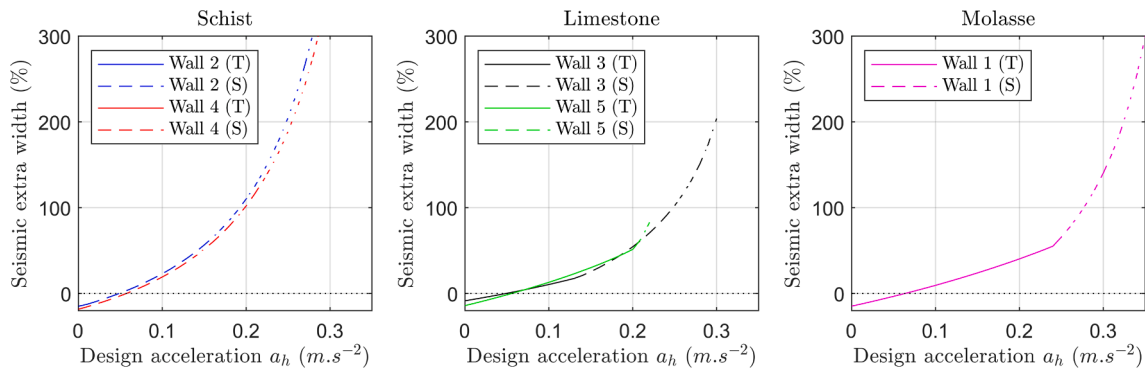


Fig. 6. Extra-width required by a seismic design compared to a non-seismic design for the studied walls. Walls are presented according to the type of stone used; a) schist; b) limestone; c) molasse (marl sandstone).

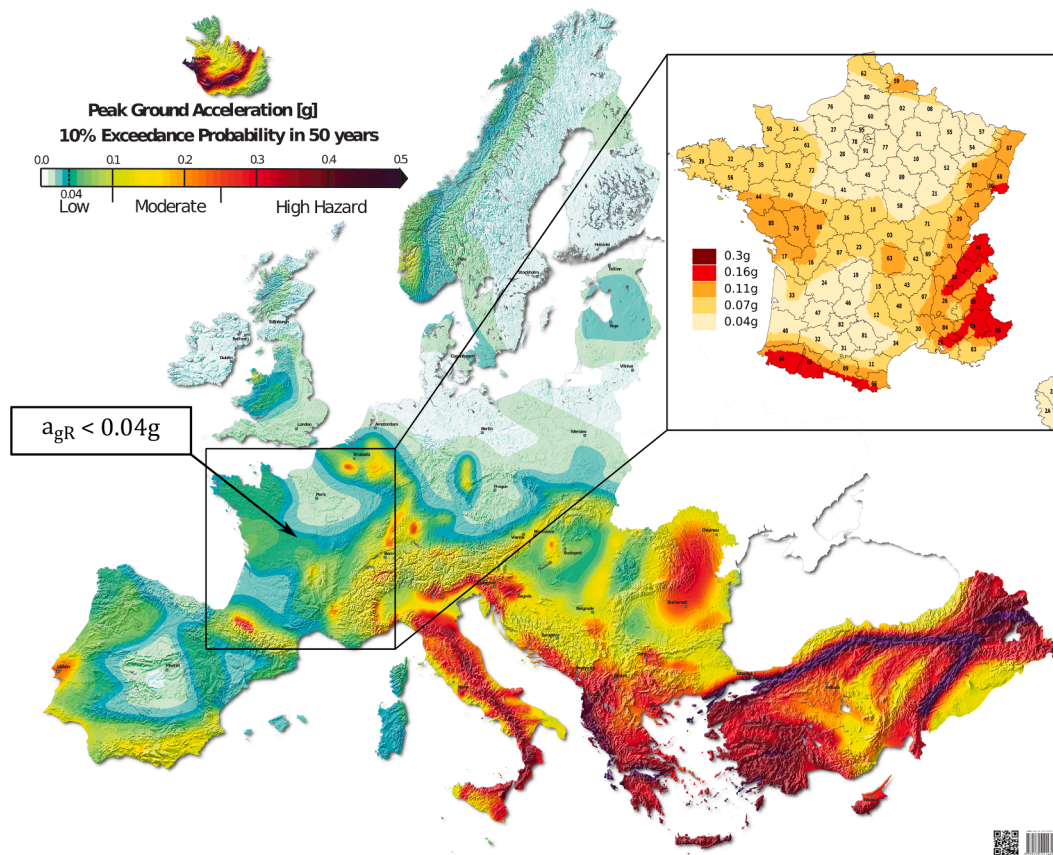


Fig. 7. European map of reference acceleration  $a_{gR}$  (return period of 475 years) according to Giardini et al. [49]. The threshold  $a_{gR} = 0.04 g$  is also highlighted in the legend. National seismic zonation maps in Eurocode 8 currently differ from this map.

French recommendations [20,21]. Table 4 details the maximum required extra-widths for each bed inclination according to different reference accelerations ( $a_{gR}$ ) representative of Europe. A non-exhaustive description of the concerned regions is also given for each reference acceleration. For most western, northern, and eastern Europe, where the reference acceleration is smaller than  $a_{gR} = 0.11g$  (low to medium seismicity), the maximum required extra-width reaches about 50%. If the wall is more resistant to sliding (not built with schist or with a non-zero bed inclination), the maximum extra-width decreases to about 35%. Finally, for reference accelerations larger than 0.25g, due to the inherent approximations of the pseudo-static approach, the maximum extra-widths exceed 100% of the non-seismic design which seems non-reasonable in practice. For these cases, the pseudo-static modelling

approach may also be inadequate, given the weak consideration of dynamics and, additionally, the fact that wall disintegration is ignored.

In conclusion, the systematic use of a stone bed inclination  $\alpha$  is recommended. Whenever possible, an external batter equal to the stone bed inclination to facilitate the construction process is also suggested. For low to medium seismic regions ( $a_{gR} < 0.11g$ ), a stone bed inclination  $\alpha$  of 10% is suitable, whereas, for larger seismic hazards ( $a_{gR} \cong 0.16-0.2g$ ), a value of 20% can help to reduce the required extra-widths significantly.

### 3.2.2. French case study

This section provides a more detailed case study for France, chosen as an illustrating example of low to medium seismicity European countries. The section helps to understand the trends and practical

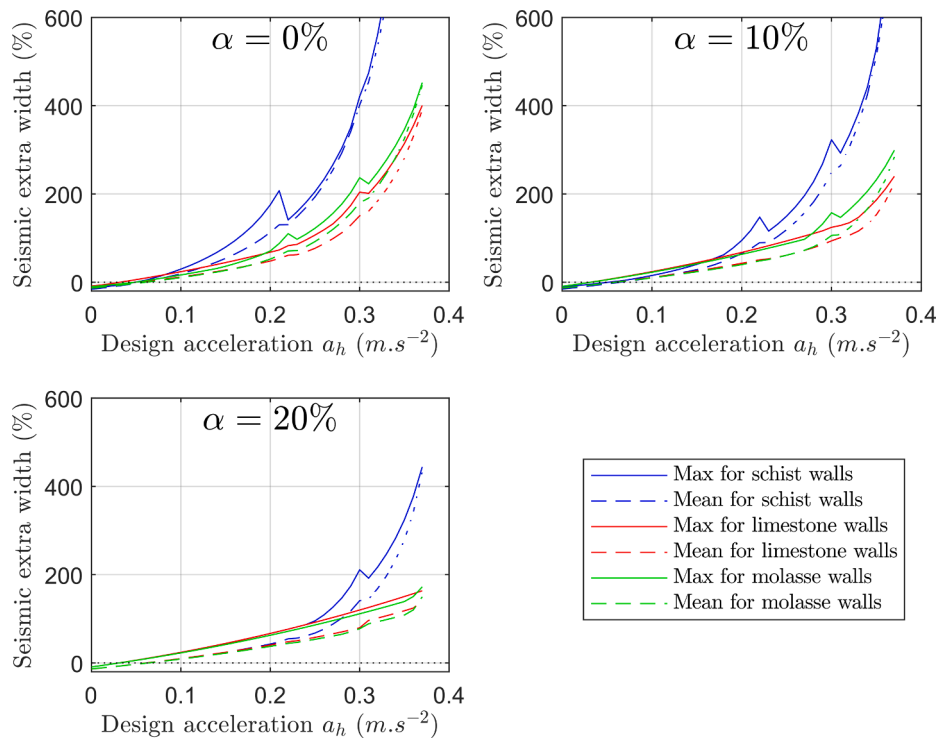


Fig. 8. Maximum (continuous line) and mean (dashed line) required extra-widths for the studied DSRWs depending on the type of stone and the stone beds inclination  $\alpha$ : a)  $\alpha = 0\%$ ; b)  $\alpha = 10\%$ ; c)  $\alpha = 20\%$ .

seismic design for DSRWs, depending on three different but typical cases for the backfill-wall condition. The first case (MAX) corresponds to the previous European study, i.e., large amplification for the soil ( $S = 1.8$ ) and a standard construction (importance factor  $\gamma_I = 1.0$ ). The second (ROCK) represents the most critical case when the DSRW is directly founded on the bedrock ( $S = 1.0$ ), considered a reference case for foundation conditions. The last one (RURAL) corresponds to walls of less importance ( $\gamma_I = 0.8$ ), built far from any road or building. In practice, according to the French regulations, these specific cases (RURAL) are not subjected to seismic regulations. However, this work gives reference values, which are helpful for DSRWs stakeholders. These three configurations are analysed according to the four seismic zones of metropolitan France ( $a_{gR} = 0.04, 0.07, 0.11$  and  $0.16g$ ), leading to a total of 12 case studies (Table 5).

Table 6 sums up the maximum (and mean) extra-widths (among the different walls and stones type) obtained for each seismic situation depending on the stone bed inclinations. In seismic zones S1 to S3, one can again note that bed inclination  $\alpha$  dramatically impacts the results; however, a bed inclination of 20% does not provide a significant increase in resistance compared with an inclination of 10% (see also

Fig. 8b-c). Therefore, as usual in the South of France, an inclination of the stone bed of 10% is recommended: seismic design requires no more than 40% extra-width (compared to a non-seismic design). In seismic zone S4, walls built with a stone bed inclination of 10% require an extra-width of 90%, which induces substantial extra costs for the wall construction. In this case, one should either use a steeper bed inclination or conduct a specific analytical computation to optimise the geometry of the DSRW. However, if the wall is built far away from roads and buildings (RURAL) and with an inclination bed of 10%, the maximum expected extra-width only reaches 50%. On the contrary, if the wall is directly founded on the bedrock (ROCK), the seismic required extra-width drops to a maximum of 30%. If both conditions are fulfilled (RURAL & ROCK), the required extra-widths do not exceed 20% (case not addressed in Table 6). Finally, the general recommendations of Table 6 (maximum values) can be readily used for practical non-seismic and seismic design of DSRWs without requiring more detailed computations.

As already noted, specific analytical computations should be carried out for the situation MAX-S4 or more critical seismic implantations instead of using the general approach with the maximum values

Table 4

Maximum extra-widths for DSRWs required by a pseudo-static seismic design compared to a non-seismic design depending on the reference acceleration ( $a_{gR}$ ). The analysis only covers DSRWs belonging to the normal class of importance ( $\gamma_I \leq 1.0$ ). According to the seismic hazard map of European countries, the second column gives the corresponding regions of each reference acceleration. The reader is referred to Figs. 7 and 8.

Reference acceleration $a_{gR}$ (design acceleration $a_{h,max}$ )	Corresponding regions in Europe	Max (and mean) extra widths		
		$\alpha = 0\%$	$\alpha = 10\%$	$\alpha = 20\%$
0.04g (0.05g)	Most Northern Europe (up to France, Germany and Poland) + Mainland Spain	6% (0%)	6% (0%)	6% (0%)
0.06g (0.07g)	Most North-Eastern Europe; first seismic zone of many countries	13% (4%)	13% (2%)	13% (2%)
0.11g (0.13g)	Most Iberia; most Northern Europe up to the north of Italy and the north of Croatia	56% (26%)	36% (19%)	36% (18%)
0.16g (0.19g)	All Northern Europe; most Eastern Europe; first seismic zones of all European countries	>100% (63%)	77% (44%)	62% (37%)
0.20g (0.24g)	All Europe except localised areas (Iceland, Portugal, Spain) and high seismic regions (Croatia-Italy-Slovenia; Bosnia-Croatia-Greece-Serbia; Bulgaria-Romania; Cyprus-Turkey)	>100% ( $\approx 100\%$ )	>100% (72%)	87% (55%)
0.25g (0.29g)	All Cyprus, Slovenia; almost all Bosnia, Bulgaria, Croatia, Greece, Italy, Romania	>100% (>100%)	>100% (>100%)	>100% (88%)
>0.25g (>0.29g)	Localised zones in Iceland; rest of Bosnia, Bulgaria, Croatia, Greece, Italy, Romania, and Turkey	>100% (>100%)	>100% (>100%)	>100% (>100%)

**Table 5**

Horizontal seismic design accelerations  $a_h$  for different critical cases (as a proportion of  $g = 9.81\text{m.s}^{-2}$ ). The vertical acceleration  $a_v$  is systematically taken equal to  $0.5 \cdot a_h$ .

	$a_{gR}$	MAX	RURAL	ROCK
Formulas used to compute $a_h$	–	$a_{h,max} = a_{gR} \cdot 1.20$	$a_{h,rural} = a_{gR} \cdot 0.96$	$a_{h,rock} = a_{gR} \cdot 0.67$
Very Low Seismic zone (S1)	0.04g	0.05g	0.04g	0.03g
Low Seismic zone (S2)	0.07g	0.09g	0.07g	0.05g
Moderate Seismic zone (S3)	0.11g	0.13g	0.11g	0.07g
Mean Seismic zone (S4)	0.16g	0.20g	0.16g	0.11g

**Table 6**

Influence of the stone bed inclination  $\alpha$  on the extra width required for seismic design. Maximum values, together with average values in parentheses, are given.

	$\alpha = 0\%$	$\alpha = 10\%$	$\alpha = 20\%$
ROCK-S1 (0.03g)	0% (0%)	0% (0%)	0% (0%)
RURAL-S1 (0.04g)	2% (0%)	2% (0%)	3% (0%)
ROCK-S2 / MAX-S1 (0.05g)	6% (0%)	6% (0%)	6% (0%)
RURAL-S2 (0.07g)	12% (4%)	12% (3%)	12% (3%)
ROCK-S3 (0.07g)	15% (6%)	15% (4%)	15% (4%)
MAX-S2 (0.09g)	20% (9%)	19% (7%)	19% (7%)
RURAL-S3 / ROCK-S4 (0.11g)	36% (17%)	27% (13%)	27% (12%)
MAX-S3 (0.13g)	61% (28%)	39% (21%)	39% (19%)
RURAL-S4 (0.16g)	89% (40%)	49% (29%)	48% (25%)
MAX-S4 (0.20g)	>100% (67%)	87% (47%)	67% (39%)

displayed in Table 6. More specifically, one should pay attention to specific parameters of the DSRW in the design that plays a critical role in the seismic computation (see full details in [40]). Apart from the positive influence of the stone bed inclination and the negative effect of the retained slope angle already highlighted, a positive internal wall batter is recommended (this is the case of a self-stable wall). To support this

recommendation, Walls 1 to 5 (with various stone types and bed inclinations) have been designed to withstand a specific seismic acceleration (0.05g, 0.10g ... and 0.35g). In a second step, each wall section geometry has been modified, adding an internal batter ( $\lambda_m = 5\%$ , 10% and 15%) but keeping the same surface area as before. It means that the total volume of stones used in that case is the same but that the geometry of the wall section is different (i.e., with a larger width at the base). Finally, the maximum acceleration withstood by the walls with an internal batter is compared to the maximum acceleration found for those without the batter (Fig. 9). The curves correspond to the average values found throughout the different walls and stones. Only positive values have been found, meaning a systematic improvement of the seismic resistance when adding an internal batter. This improvement is particularly significant for walls with non-zero stone bed inclination and low (S2) to moderate (S3) seismic hazard regions.

To conclude, in zone S2, no DSRW extra-width is required to fulfil a seismic design if both an inclination bed of 10% and an internal batter of at least 10% are used. This means that an adequate choice for the wall geometry compensates for the extra resistance required to satisfy a seismic design in case of low seismicity.

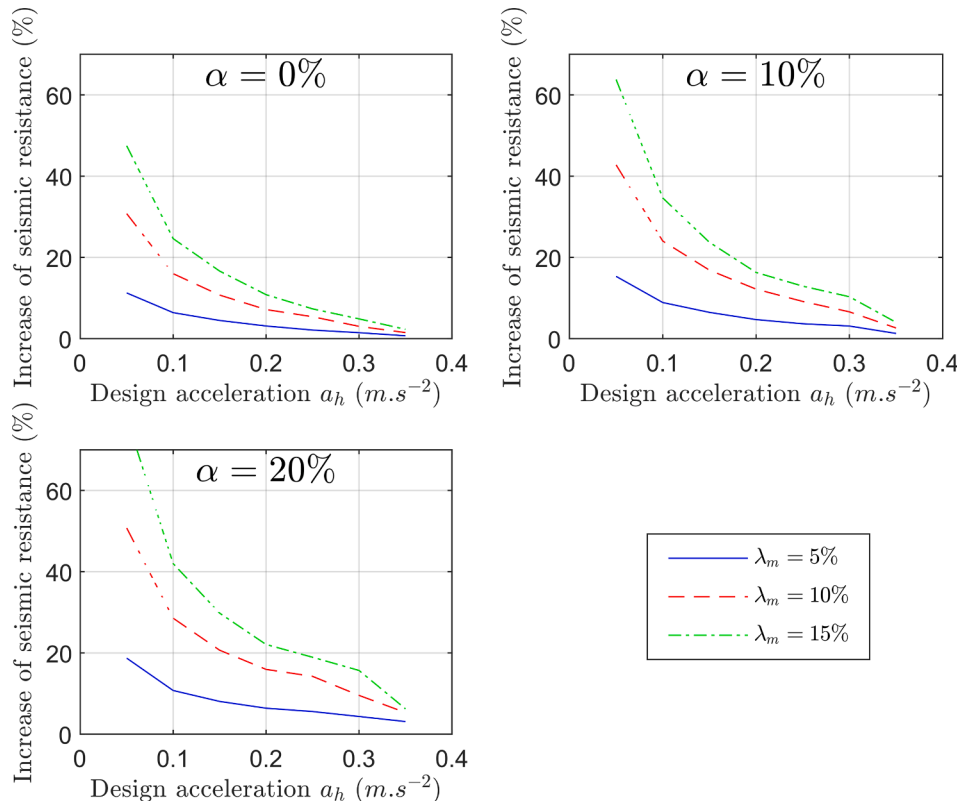


**Fig. 9.** Effect of the internal batter  $\lambda_m$  (keeping the same area for the wall section) on the seismic resistance of a DSRW for different bed inclinations a)  $\alpha = 0\%$ ; b)  $\alpha = 10\%$ ; c)  $\alpha = 20\%$ .

#### 4. Conclusions

The present study addresses non-seismic and seismic designs of Dry Stone Retaining Walls (DSRWs) according to the European standards (Eurocodes) used for conventional retaining walls while proposing an adapted methodology (e.g. including internal failure of DSRW). It has been shown that the current French recommendations for the non-seismic design of DSRWs comply with Eurocode 7 (geotechnical engineering) standards being slightly more conservative than the latter. Moreover, in very low seismic zones ( $a_h < 0.05g$ ), non-seismic limit states are the most critical states for the design of DSRWs, which confirms that a seismic design is not required in these regions [29]. This is generally not the case in zones of higher seismicity where the seismic design according to Eurocode 8 (seismic engineering) standard is almost always the most critical.

The study revealed different geometrical optimisation options for DSRWs. It is highly recommended to use systematically: i) a bed inclination of at least 10%; ii) a flat retained backfill; iii) and a positive internal batter of at least 10%. These three geometric parameters have a significant impact on seismic design. If these recommendations are followed in low seismic zones (up to  $a_h = 0.08g$ ), there is also no increase in dimensions to fulfil a seismic design.

The pseudo-static approach generally gives practical global recommendations for low to moderate seismic hazard zones (up to  $a_h = 0.2g$ ). In addition, a specific geometrically optimised (as stated above) pseudo-static design can still produce affordable recommendations in more critical cases (up to  $a_h = 0.3g$ ). However, for higher design acceleration or particularly critical cases, the pseudo-static approach for the seismic design leads to values higher than 50% for the extra-widths. In this case, dynamic time history computations are recommended to obtain more accurate results that account for wall disintegration failure. Indeed, this failure mode may be critical for high seismicity areas, particularly if combined with poor execution conditions.

Finally, as an example illustrating European countries, France is used as a case study of seismic design applied to DSRWs in low to moderate seismicity areas. In metropolitan France, where many DSRWs can be found, the expected extra-width provided by seismic design does not exceed 40% for walls located in low seismic zones presenting a stone bed inclination of 10%, in case the foundation is not on the bedrock. In the same conditions, walls built in moderate seismic hazard zones need either a stone bed inclination of 20% or a specific analytical computation to optimise the section. Finally, walls directly founded on the bedrock, in the case of low and moderate seismicity areas, require a maximum of 30% extra width to fulfil a seismic design.

#### Funding

This work was partly financed by FCT / MCTES through national funds (PIDDAC) under the R&D Unit Institute for Sustainability and Innovation in Structural Engineering (ISISE), under reference UIDB / 04029/2020. This study has also been partly funded by the STAND4-HERITAGE project (New Standards for Seismic Assessment of Built Cultural Heritage) that has received funding from the European Research Council (ERC) under the European Union's Horizon 2020 research and innovation programme (Grant agreement No. 833123), as an Advanced Grant. In addition, the authors want to acknowledge the French Ministry of Education and Research for their financial support through a PhD grant attributed to the first author. The opinions and conclusions presented in this paper are those of the authors and do not necessarily reflect the views of the sponsoring organisations.

#### Data availability

The data arising from the analytical simulations presented in the paper is not available publicly.

#### CRediT authorship contribution statement

**Nathanaël Savalle:** Investigation, Formal analysis, Writing – original draft. **Christine Monchal:** Methodology, Resources, Investigation. **Eric Vincens:** Funding acquisition, Writing – original draft, Methodology, Supervision. **Sten Forcioli:** Resources, Writing – review & editing, Methodology. **Paulo B. Lourenço:** Supervision, Funding acquisition, Writing – review & editing.

#### Declaration of Competing Interest

The authors declare that they have no known competing financial interests or personal relationships that could have appeared to influence the work reported in this paper.

#### Data availability

Data will be made available on request.

#### References

- [1] Villemus B, Morel J-C, Boutin C. Experimental assessment of dry stone retaining wall stability on a rigid foundation. *Eng Struct* 2006;29(9):2124–32. <https://doi.org/10.1016/j.engstruct.2006.11.007>.
- [2] Colas A-S, Morel J-C, Garnier D. Full-scale field trials to assess dry-stone retaining wall stability. *Eng Struct* 2010;32(5):1215–22. <https://doi.org/10.1016/j.engstruct.2009.12.047>.
- [3] Colas A-S, Morel J-C, Garnier D. Assessing the two-dimensional behaviour of drystone retaining walls by full-scale experiments and yield design simulation. *Géotechnique* 2013;63(2):107–17. <https://doi.org/10.1680/geot.10.P.115>.
- [4] Mundell C, McCombie P, Bailey C, Heath A, Walker P. Limit-equilibrium assessment of drystone retaining structures. *Proc Inst Civ Eng (Geotech Eng)* 2009;162(4):203–12. <https://doi.org/10.1680/jgeot.2009.162.4.203>.
- [5] Alejano LR, Veiga M, Taboada J, Díez-Farto M. Stability of granite drystone masonry retaining walls: I. Analytical design. *Géotechnique* 2012;62(11):1013–25. <https://doi.org/10.1680/geot.10.P.112>.
- [6] Colas A-S, Morel J-C, Garnier D. Yield design modelling of dry joint retaining structures. *Constr Build Mater* 2013;41:912–7. <https://doi.org/10.1016/j.conbuildmat.2012.07.019>.
- [7] Terrade B, Colas A-S, Garnier D. Upper bound limit analysis of masonry retaining walls using PIV velocity fields. *Meccanica* 2018;53(7):1661–72. <https://doi.org/10.1007/s11012-017-0673-6>.
- [8] Harkness RM, Powrie W, Zhang X, Brady KC, O'Reilly MP. Numerical modelling of full-scale tests on drystone masonry retaining walls. *Géotechnique* 2000;50(2):165–79. <https://doi.org/10.1680/geot.2000.50.2.165>.
- [9] Powrie W, Harkness RM, Zhang X, Bush DI. Deformation and failure modes of drystone retaining walls. *Géotechnique* 2002;52(6):435–46. <https://doi.org/10.1680/geot.2002.52.6.435>.
- [10] Claxton M, Hart RA, McCombie PF, Walker PJ. Rigid block distinct-element modelling of dry-stone retaining walls in plane strain. *ASCE J Geotech Geoenviron Eng* 2005;131(3):381–9. [https://doi.org/10.1061/\(ASCE\)1090-0241\(2005\)131:3\(381\)](https://doi.org/10.1061/(ASCE)1090-0241(2005)131:3(381)).
- [11] Walker P, McCombie P, Claxton M. Plane strain numerical model for drystone retaining walls. *Proc Inst Civ Eng – Geotech Eng* 2007;160(2):97–103. <https://doi.org/10.1680/jgeot.2007.160.2.97>.
- [12] Alejano LR, Veiga M, Gómez-Márquez I, Taboada J. Stability of granite drystone masonry retaining walls: II. Relevant parameters and analytical and numerical studies of real walls. *Géotechnique* 2012;62(11):1027–40. <https://doi.org/10.1680/geot.10.P.113>.
- [13] Oetomo JJ, Vincens E, Dedecker F, Morel J-C. Modeling the 2D behavior of dry-stone retaining walls by a fully discrete element method. *Int J Numer Anal Meth Geomech* 2016;40(7):1099–120. <https://doi.org/10.1002/nag.2480>.
- [14] Li Z, Zhou Y, Guo Y. Upper-Bound Analysis for Stone Retaining Wall Slope Based on Mixed Numerical Discretization. *Int J Geomech* 2018;18(10):1–14. [https://doi.org/10.1061/\(ASCE\)GM.1943-5622.0001247](https://doi.org/10.1061/(ASCE)GM.1943-5622.0001247).
- [15] Pulatsu B, Kim S, Erdogmus E, Lourenço PB. Advanced analysis of masonry retaining walls using mixed discrete-continuum approach. *Proc Inst Civ Eng-Geotech Eng* 2020;1–13. <https://doi.org/10.1680/jgeen.19.00225>.
- [16] Mundell C, McCombie P, Heath A, Harkness J. Behaviour of drystone retaining structures. *Proc Inst Civ Eng (Struct Build)* 2010;163(1):3–12. <https://doi.org/10.1680/stbu.2009.163.1.3>.
- [17] Le HH, Garnier D, Colas A-S, Terrade B, Morel J-C. 3D homogenised strength criterion for masonry: Application to drystone retaining walls. *J Mech Phys Solids* 2016;95:239–53. <https://doi.org/10.1016/j.jmps.2016.05.021>.
- [18] Le HH, Morel J-C, Colas A-S, Terrade B, Garnier D. Assessing the Three-Dimensional Behaviour of Dry Stone Retaining Walls by Full-Scale Experiments. *Int J Arch Heritage* 2020;14(9):1373–83. <https://doi.org/10.1080/15583058.2019.1607627>.

- [19] Quezada J-C, Vincens E, Moutherde R, Morel J-C. 3D failure of a scale-down dry stone retaining wall: a DEM modelling. *Eng Struct* 2016;117:506–17. <https://doi.org/10.1016/j.engstruct.2016.03.020>.
- [20] CAPEB, ABPS, Murailleurs de Provence, CBPS, CMA84, and ENTPE, *Pierres sèches: guide de bonnes pratiques de construction de murs de soutènement*. ENTPE, 2008.
- [21] ENTPE, Artisans Bâisseurs en Pierre Sèche (ABPS), Ecole des Ponts ParisTech, IFSTTAR, and Fédération Française du Bâtiment (FFB), *Technique de construction des murs en pierre sèche : Règles professionnelles*. ENTPE, Artisans Bâisseurs en Pierre Sèche (ABPS), 2017.
- [22] AFPS, *Recommandations AFPS 90*. Presses des Ponts et Chaussées Paris, 1990.
- [23] H.H. Le, 'Stabilité des murs de soutènement routiers en pierre sèche : Modélisation 3D par le calcul à la rupture et expérimentation échelle 1', PhD Thesis, Ecole Nationale des Travaux Publics de l'Etat (ENTPE), 2013.
- [24] AFNOR, *NF EN 1997-1:2005 (Eurocode 7) : Geotechnical design - Part 1: General rules*, vol. 7, 8 vols., 2005.
- [25] AFNOR, NF P 94-281: Justification des ouvrages géotechniques - Normes d'application nationale de l'Eurocode 7 - Ouvrages de soutènement - Murs, 2014.
- [26] AFNOR, NF P 94-261: Justification des ouvrages géotechniques - Normes d'application nationale de l'Eurocode 7 - Fondations superficielles, 2014.
- [27] Savalle N, Vincens E, Hans S. Pseudo-static scaled-down experiments on dry stone retaining walls: Preliminary implications for the seismic design. *Eng Struct Sep*. 2018;171:336–47. <https://doi.org/10.1016/j.engstruct.2018.05.080>.
- [28] AFNOR, *NF EN 1998-5:2005 (Eurocode 8): Design of structures for earthquake resistance - Part 5: Foundations, retaining structures and geotechnical aspects*, vol. 8, 8 vols, 2005.
- [29] AFNOR, *NF EN 1998-1:2005 (Eurocode 8): Design of structures for earthquake resistance - Part 1: General rules, seismic actions and rules for buildings*, vol. 8, 8 vols, 2005.
- [30] B. Villemus, *Etude des Murs de Soutènement en Maçonnerie de Pierre Sèches*, PhD Thesis, Ecole Nationale des Travaux Publics de l'Etat (ENTPE), 2004.
- [31] C.A. Coulomb, *Essai sur une application des regles des maximis et minimis a quelques problemes de statique relatifs a l'architecture*, vol. 7. 1773.
- [32] Okabe S. General theory on earth pressure and seismic stability of retaining wall and dam. *Proc Civil Engrg Soc, Japan* 1924;10(6):1277–323.
- [33] Mononobe N, Matsuo H. On Determination of Earth Pressures during Earthquakes. *World Engineering Conference* 1929;9:177–85.
- [34] Savalle N, Vincens E, Lourenço PB. Pseudo-static analytical model for the static and seismic stability of dry stone retaining walls, Lisbon, Portugal; 2022. doi: 10.11159/icgre22.138.
- [35] Ishibashi I, Fang Y-S. Dynamic earth pressures with different wall movement modes. *Soils Found* 1987;27(4):11–22.
- [36] Ichihara M, Matsuzawa H. Earth pressure during earthquake. *Soils Found* 1973;13(4):75–86.
- [37] Savalle N, Vincens É, Hans S. Experimental and numerical studies on scaled-down dry-joint retaining walls: Pseudo-static approach to quantify the resistance of a dry-joint brick retaining wall. *Bull Earthq Eng Jan*. 2020;18:581–606. <https://doi.org/10.1007/s10518-019-00670-9>.
- [38] Colas A-S, Morel J-C, Garnier D. Yield design of dry-stone masonry retaining structures - Comparisons with analytical, numerical, and experimental data. *Int J Numer Anal Methods Geomech* 2008;32(14):1817–32. <https://doi.org/10.1002/nag.697>.
- [39] Colas A-S. 'Mécanique des murs de soutènement en pierre sèche : Modélisation par le calcul à la rupture et expérimentation échelle 1', PhD Thesis. Ecole Nationale des Travaux Publics de l'Etat (ENTPE); 2009.
- [40] Savalle N. Comportement sismique des murs de soutènement de talus en pierre sèche, PhD Thesis. Lyon; 2019. [Online]. Available: 10.5281/zenodo.4288880.
- [41] Wang J, Thusyanthan I. Evaluating foundation design concepts of Eurocode 7 & 8; 2008.
- [42] Pecker A, Pender M. Earthquake resistant design of foundations: new construction; 2000.
- [43] Koseki J, Bathurst RJ, Guler E, Kuwano J, Maugeri M. Seismic stability of reinforced soil walls. In: *Proc of 8th International Conference on Geosynthetics*, vol. 1; 2006. p. 51–77.
- [44] Fardis MN. *Seismic design, assessment and retrofitting of concrete buildings: based on EN-Eurocode 8*, vol. 8. Springer Science & Business Media; 2009.
- [45] Savalle N, Blanc-Gonnet J, Vincens E, Hans S. Dynamic behaviour of drystone retaining walls: shaking table scaled-down tests. *Europ J Environ Civ Eng* 2022;26(10):4527–47.
- [46] Savalle N, Vincens E, Hans S, Lourenço PB. Dynamic Numerical Simulations of Dry-Stone Retaining Walls: Identification of the Seismic Behaviour Factor. *Geosciences* 2022;12(6):252. <https://doi.org/10.3390/geosciences12060252>.
- [47] Brady KC, Kavanagh J. Analysis of the stability of masonry-faced earth retaining walls. *Transport Res Laboratory Crowthorne* 2002.
- [48] Colas A-S, Morel J-C, Garnier D. 2D modelling of a dry joint masonry wall retaining a pulverulent backfill. *Int J Numer Anal Meth Geomech* 2010;34(12):1237–49. <https://doi.org/10.1002/nag.855>.
- [49] Giardini D, Wössner J, Danciu L. Mapping Europe's seismic hazard. *Eos, Trans Am Geophys Union* 2014;95(29):261–2. <https://doi.org/10.1002/2014EO290001>.